Journal of Naval Architecture and Marine Engineering
June, 2023
https://doi.org/10.3329/jname.v20i1.58298 *https://www.banglajol.info*

STRESS-STRAIN ANALYSIS OF STRUCTURAL DISCONTINUITIES ASSOCIATED WITH SHIP HULLS

Kazi Naimul Hoque[1*], Md. Shahidul Islam[1]

[1]Department of Naval Architecture and Marine Engineering, Bangladesh University of Engineering and Technology (BUET), Dhaka-1000, Bangladesh, kazinaim@name.buet.ac.bd*, shahid777@name.buet.ac.bd

Abstract:

The finite element method (FEM) is already well-established as a strong and widely used numerical analytical methodology for determining solutions to a wide variety of structural mechanics issues. One of the most significant subjects in the design of not only ships but also airplanes and other structures is the configuration of plate-type structures. When these plate-type structures are subjected to in-plane loading, the plane stress formulation can be used for finite element analysis to reduce the computational cost. A reliable finite element code is developed in C++ program using an object-oriented approach. This approach reduces the complexity of coding, keeping data available for further analysis like mesh refining, optimization process, and data visualization very effectively. This article primarily focuses on the fundamental concepts of FEM for finding solutions to two-dimensional plane stress and plane strain problems to evaluate stresses such as normal stress, shear stress, and von Mises stress at the four integration points (gauss points) of quadrilateral elements for various sections of ship structures (especially at the most vulnerable areas), such as a plate with holes, plate with bracket and holes, and plate with fillets. With the aid of commercial finite element analysis software, the analysis findings of gauss point stresses for different ship sections produced from the developed program are validated.

Keywords: Plane stress; plane strain; structural discontinuities; finite element analysis; von Mises stress; object oriented programming.

NOMENCLATURE

Q	global displacement vector	σ_Y	yield stress
F	global load vector	σ_x	normal stress along x-direction
u, v	Components of displacement for a two-dimensional body	σ_y	normal stress along y-direction
q	element displacement vector	τ_{xy}	shear stress
ξ-, η	natural coordinates	σ_{misses}	von Mises stress
D	stress strain displacement matrix	t	thickness of the plates
B	element strain displacement matrix	υ	Poisson's ratio
K	element stiffness matrix	d	diameter of the hole
E	modulus of elasticity	r	bracket radius
σ	stress	L	length of the plate
ε	strain		

1. Introduction

A structural discontinuity is a break or gap in a structural component that causes it to behave differently when it is loaded. One of the most significant topics in the construction of ships, airplanes, and automobiles is how to configure structures with discontinuities. A structural discontinuity occurs when the cross-section of a structural member changes abruptly, such as deck openings like as hatch and machinery openings, access openings on side walls, cutouts

1813-8535 (Print), 2070-8998 (Online) Received on: Feb., 2022

in the web plate, oil hole in crankshaft, and so on. Because structural discontinuities change a structure's stress distribution, they also cause stresses around the crack's tip or along the hole's edge. These locations of high stress are of particular significance throughout the design and testing process; as a result, an exact approach must be used to study the impacts of these discontinuities so that engineers can design around them. Finite element analysis (FEA) is a well-known structural analysis method that may be used to analyze for structural discontinuity issues (Kar et al., 2008; Parunov et al., 2010; and Islam et al., 2017).

The significance of fatigue cracks and corrosion in tankers was thoroughly investigated by Bea et al. (Bea et al., 1995). The structural integrity of a hull girder penetration and a short longitudinal bulkhead were examined using finite element modeling by Baumann (Baumann, 1997). However, there is very few research that can simulate how corrosion and fatigue cracking influence the structural integrity of ship hull structures (Soares and Garbatov, 1998). Niu (Niu, 1998) conducted considerable study on stress analysis in case of aircraft structure. The difficulty of modeling arises from the high degree of uncertainty about how corrosion and fatigue cracking would affect the structural integrity of a ship's hull. Probabilistic models must be employed to evaluate the effects of corrosion and fatigue fractures because of their random spatial distribution on a structure, their time-dependent growth, and their interactions in service. The widespread use of sophisticated, efficient computational techniques, frequently based on the finite element method, has increased knowledge of the application and significance of stress analysis. It is common practice to compute a mechanical device's stress analysis, which includes areas under extreme strain. Most experimental approaches to stress analysis have been replaced by more flexible and cost-effective computer techniques. However, these analyses can now be performed with a high level of precision because of the development of the finite element approach. Strebel and Moet (Strebel and Moet, 1993) conducted considerable research on plane strain and plane stress problems.

Forde et al., Zimmermann et al., and Dubois-Pelerin et al. reported the pioneering attempts to develop finite element software architecture (Forde et al., 1990; Zimmermann et al., 1992; Dubois-Pelerin et al., 1992). Fenves, Miller, Desjardins, and Fafard added more insights (Fenves, 1990; Miller, 1991; Desjardins and Fafard, 1992). A significant amount of interest was generated by Mackerle's work on the integration of object-oriented concepts and finite element programming (Mackerle, 2000). The object-oriented finite element programming framework has been extensively investigated by Martha (Martha, 2002). The application of object-oriented techniques to the finite element approach led to the development of a code that was incredibly flexible, easily comprehendible, and expandable. Research on the two-dimensional plane stress and plane strain analysis of structural discontinuities in ship building structures was done by Hoque (Hoque, 2016). Using finite element analysis, the topology of an oil tanker bulkhead susceptible to hydrostatic loads was addressed (Islam and Paul, 2021). Numerous research has been done on the development of fractures and corrosion in maritime structures constructed of marine materials (Presuel-Moreno et al., 2022, 2018; Presuel-Moreno and Hoque, 2023, 2019; Hoque, 2020). Edholm used the Python programming language to do finite element analysis for the visualization of quadrilateral and triangular meshes (Edholm, 2013).

In this paper, object-oriented programming (OOP) technique is used. The major advantage of adopting an object-oriented approach is that the program expansion is simpler and more natural, as new implementations have a minimum impact in the existing code. Thus, the reuse of code is maximized. Moreover, compared to the classical, structured programming, the use of the OOP leads to a closer integration between theory and computer implementation. The OOP is particularly useful in the development of large and complex programs, as the finite element methods that should handle different element types, constitutive models, and analysis algorithms. This study focuses on the principles of FEM for analyzing stresses such as normal stress, shear stress, and von Mises stress at the four integration points (gauss point) for different members of ship structures such as plate with holes, plate with bracket and holes, and plate with fillets. The OOP method is used to develop a finite element program for four node quadrilateral elements to analyze structural discontinuity problems for various ship structures. The study findings of gauss point stresses for several models obtained from the developed program are validated using the commercial finite element analysis software SIMULIA ABAQUS.

2. Basic Formulation

In structural mechanics, the Finite Element Method is the most widely used discretization approach. The subdivision of a region into discrete (non-overlapping) components of simple geometry, known as finite elements or elements for

short, is the core principle of FEM. Linear or quadratic triangles and quadrilaterals are the most basic elements in two-dimensional modeling. Each node in a two-dimensional space is allowed to move in two directions. Each node has two degrees of freedom as a result. Therefore, the x and y displacement components of node j are Q_{2j-1} and Q_{2j}, respectively. Furthermore, the global displacement vector may be written as

$$\{Q\} = [Q_1, Q_2, \ldots\ldots\ldots, Q_N]^T \quad (1)$$

and global load vector,

$$\{F\} = [F_1, F_2, \ldots\ldots\ldots, F_N]^T \quad (2)$$

where N is the number of degrees of freedom (d.o.f.), which is defined as the nodes' flexibility to move in permitted numbers of direction. As the nodes are allowed to move in both the $\pm x$ and $\pm$y directions (translatory movement) in a two-dimensional issue, each node has two degrees of freedom.

2.1 Formulation of four-node quadrilateral element matrices

A general four-node quadrilateral element is considered as shown in Figure 1, which has local nodes numbered as 1, 2, 3 and 4 in a counterclockwise fashion and (x_i, y_i) are the coordinates of node i. The vector $\{q\}= [q_1, q_2, \ldots\ldots q_8]^T$ represents the element displacement vector. The displacement of an interior point P located at (x, y) can be expressed as

$$\{u\} = [u\,(x, y),\, v\,(x, y)]^T$$

To develop the shape functions, let us consider a master element (Figure 2) that has a square shape and being defined in ξ-, η- coordinates (or natural coordinates). The Lagrange shape functions, where i = 1, 2, 3 and 4, are defined such that N_i is equal to unity at node i and is zero at other nodes. In particular:

$$N_1 = \begin{cases} 1, & at\ node\ 1 \\ 0, & at\ node\ 2,\ 3\ and\ 4 \end{cases} \quad (3)$$

Now, the requirement that $N_1 = 0$ at nodes 2, 3 and 4 is equivalent to requiring that $N_1 = 0$ along edges $\xi = +1$ and $\eta = +1$ (Figure 2).

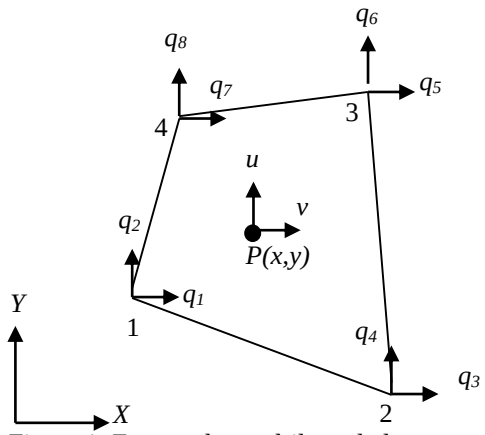

Figure 1: Four-node quadrilateral element

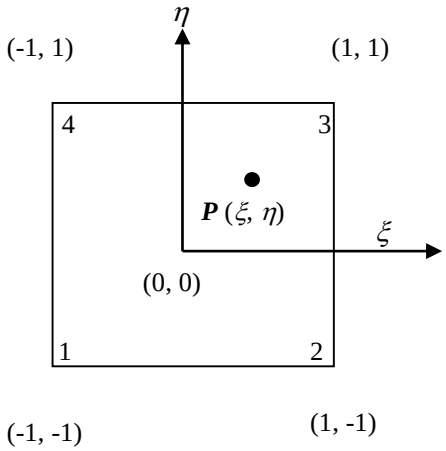

Figure 2: The quadrilateral element in ξ, η space (master element)

Shape function can be expressed as S_F to represent differently. All the four shape functions can be written as

$$N_1 = \frac{1}{4}(1-\xi)(1-\eta) \qquad N_2 = \frac{1}{4}(1+\xi)(1-\eta)$$
$$N_3 = \frac{1}{4}(1+\xi)(1+\eta) \qquad N_4 = \frac{1}{4}(1-\xi)(1+\eta) \tag{4}$$

2.2 Treatment of boundary conditions

The penalty approach is used to deal with the correct boundary condition and get the equilibrium equations. Those corresponding to equilibrium configurations have the lowest total potential energy of all possible displacements that satisfy the boundary conditions of a structural system. The finite element equations can be written in matrix form by applying these boundary conditions,

$$[K]\{Q\} = \{F\} \tag{5}$$

where, $[K]$ and $\{F\}$ are the modified stiffness and load matrices. The conjugate gradient technique is used to solve the matrices.

2.3 Element stress calculation

The penalty approach is used to solve Equation (5) for the displacement vector $\{Q\}$. The boundary condition can be regarded appropriately provided because the matrix $[K]$ is nonsingular. Once $\{Q\}$ has been determined, the element stress can be assessed using the equation obtained from Hooke's law.

$$\{\sigma\} = [E][B]\{q\} \tag{6}$$

where [B] is the element strain-displacement matrix which can expressed as the product of [A] and [G] matrices and {q} is the element displacement vector for each element, which is extracted from {Q}, using element connectivity information.

Von Mises stress is a geometrical combination of all stresses acting at a certain location (normal stress in two-directions and shear stress). When the von Mises stress at a given location exceeds the yield strength, the material yields there. The material ruptures at that place if the von Mises stress exceeds the ultimate strength. The von Mises stress σ_{mises} should be smaller than the yield stress σ_Y of the material, according to the failure criterion.

The criteria in the inequality form may be written as

$$\sigma_{mises} \leq \sigma_Y$$

The von Mises stress σ_{mises} is given by,

$$\sigma_{mises} = \sqrt{\left(\sigma_x + \sigma_y\right)^2 - 3\left(\sigma_x\sigma_y - \tau_{xy}^2\right)} \tag{7}$$

3. Research Methodology

Object-oriented programming (OOP) is particularly useful in the development of large and complex programs. The major advantage of adopting an object-oriented approach is that the program expansion is simple and natural. Compared to classical, structured programming, the use of the OOP leads to a close integration between theory and computer implementation.

3.1 Object-oriented concepts

In programming, the consumer-supplier (or master-slave) paradigm may aid comprehension of OOP ideas. A consumer and a supplier are two key aspects in the programming activity. In the current situation, a global FEM

algorithm might be viewed as a consumer. The assembling of the global stiffness matrix, for example, seeks the services of specific procedures that compute individual finite element stiffness matrices (as a consumer). The suppliers to the global algorithm are the routines that compute these matrices. There are several providers for different types of finite elements. In traditional (procedural) programming, the global algorithm is responsible for selecting functions that work well with the data that it controls. As a result, the consumer gets complete visibility into the supplier's methods as well as the data necessary to carry out the activities. Each action must be completed in a certain way by the consumer, who calls a specific routine for each sort of element.

One of the main concepts in OOP, called Encapsulation, changes the consumer-supplier relationship in a global algorithm. OOP creates a fence protecting the supplier's data, encapsulating it. The responsibility for choosing the operator (procedure) that is type compatible with the kind of operand (data) has moved from the consumer to the supplier. In OOP, a Class is a set of methods and templates of data, and an Object is an instance of that class. Consumer deals only with global algorithms and abstract data types, calling methods (generic procedures) that manipulate objects. Supplier deals with the procedures that implement the methods of a class and its objects.

3.2 Finite element programming

In the case of a FEMOOP program's class structure, the calculations in a nonlinear finite element analysis are taken place at three different levels: structure, element, and integration point. The algorithms used to investigate the problem are represented at the structural (or global) level (e.g., linear static, linearized buckling, linear dynamic, nonlinear path-following, and nonlinear dynamic). These algorithms are written in terms of global vectors and matrices, and they are unaffected by the elements and materials employed in the study.

The computation of element vectors and matrices (e.g., internal force vector and stiffness matrix) necessary to assemble the global vectors and matrices utilized by the analysis algorithms is the major work done at the element level. The technique used to (globally) assess the model has no bearing on the calculation of these vectors and matrices.

There is bidirectional connection between the global and element levels. The computation of global vectors and matrices adding up the element contributions occurs in the upward direction, whereas the extraction of element displacements from the global displacement vector occurs in the downward direction.

Finally, at the integration point level, the stress vector and tangent constitutive matrices are computed. These values are employed in the computation of element vectors and matrices, although they are independent of element formulation if the primary input data for stress computation is strain components.

Object-oriented and generic programming capabilities allow a programmer to write fewer lines of code while yet supporting an ongoing code development process. For example, one version of the preconditioned conjugate gradient method program can be used to store full (every entry of a matrix), banded (zero entries outside of a band along the main diagonal are not stored to save memory), and sparse (only non-zero entries of a matrix are stored to save memory) matrices, as well as real and complex single, double, and long double precisions. It may be possible to achieve it with six different versions of code, but it will be inefficient. This circumstance may still be handled by the same software for conjugate gradient technique without any changes.

The problem domain must be discretized into discrete (non-overlapping) components of basic geometry called finite elements or elements for short to perform finite element analysis. There are primarily two types of elements in two-dimensional finite element analyses: triangular and quadrilateral elements. Four node quadrilateral elements are employed in this paper's study.

A short description of the object-oriented code used for this research is summarized below.

Two classes are created in the present code: Node and Element. Node class has several attributes like coordinates, displacements, boundary conditions, loads etc. Member functions read and calculate these attributes. Similarly, the Element class has several attributes like member nodes, element thickness, material properties etc. The member functions of this class also read and calculate these attributes. Then an array of objects of these classes are created from which global stiffness matrix and global load vector are assembled. Using the penalty approach of handling boundary conditions, nodal displacements and elemental stresses are evaluated.

The flow chart of the developed program is shown in Figure 3.

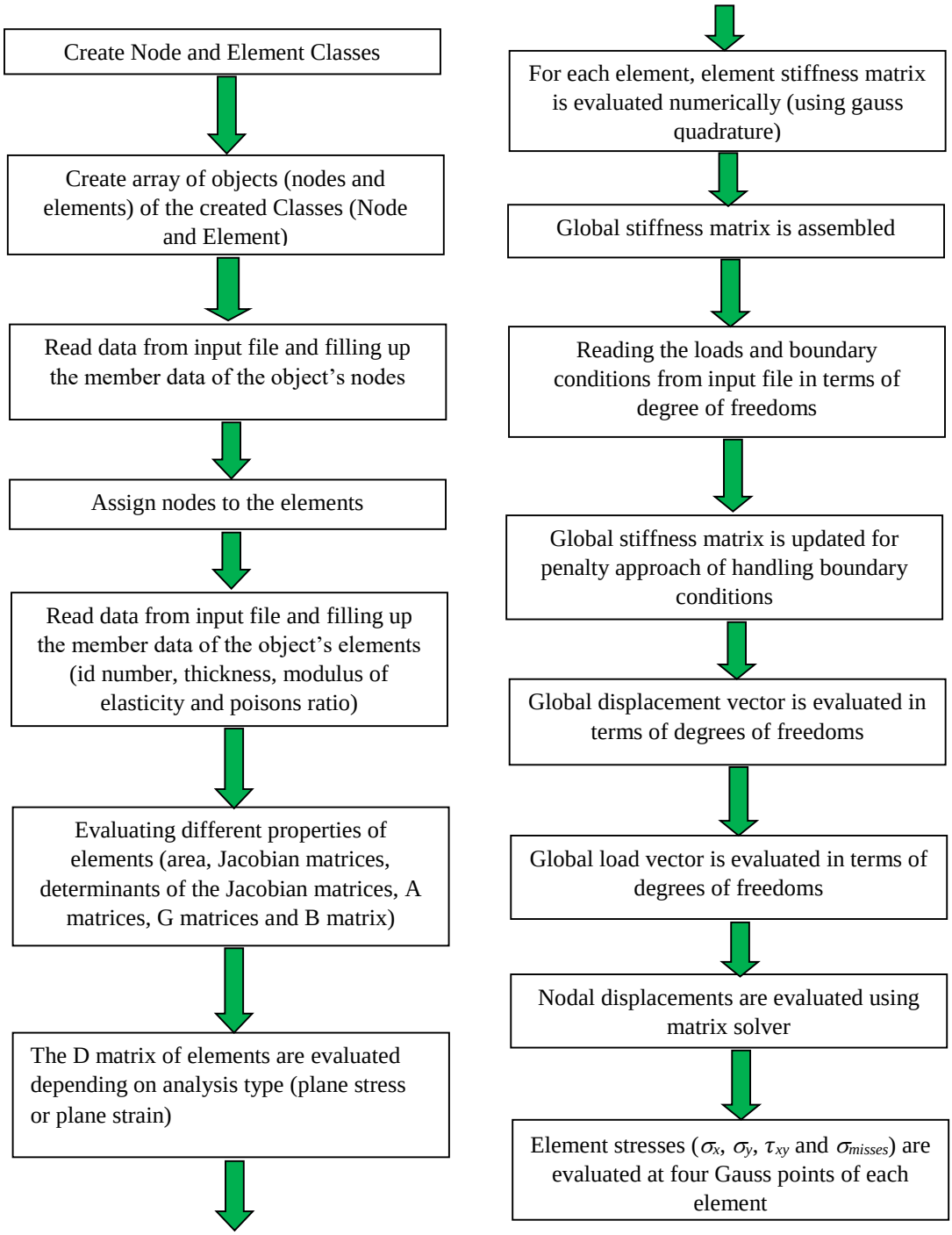

Figure 3: Flow chart of the developed program

3.3 Reasons for choosing quadrilateral element

Previous research has looked at the convergence properties of two-dimensional solutions to elastic continuum problems employing both quadrilateral and triangular elements. According to these studies, the basic shape of the element, element distortion, and polynomial order of the element, completeness of polynomial functions, integration techniques, and material incompressibility are all important factors that affect convergence characteristics of finite element solutions. When compared to bilinear quadrilaterals, simplex triangular components are often thought to be

inferior. Quadrilateral elements are favored for two-dimensional meshes while hexahedral elements are chosen for three-dimensional meshes due to higher accuracy and efficiency. This predilection is evident in structural analysis, and it appears to apply to other engineering fields as well. However, triangular components with higher order displacement assumptions are often acknowledged as providing sufficient accuracy and convergence properties. Mesh locking owing to material incompressibility, on the other hand, is a major drawback in triangular components.

4. Results and Discussion

In this investigation, finite element analysis software SIMULIA ABAQUS 13.3 version is utilized. Pre-processing or modeling, processing or finite element analysis, and post-processing or creating reports, image, animation, and other output files are all part of a comprehensive finite element analysis. Pre-processing, post-processing, and monitoring the solver's processing step are all possible using finite element analysis software. Different issues of plane stress and plane strain analysis linked to ship structures are investigated in this part with proper boundary conditions and loadings using finite element analysis software. Images and a report file from the finite element analysis program are used to display the findings.

The developed program's output file is used to analyze several types of two-dimensional plane stress and plane strain issues. Normal stresses, shear stress, and von Mises stress are primarily investigated at the four integration points for the most susceptible areas of various structural components of a ship. Therefore, the stress data from the developed program and the finite element analysis software are compared. These results' percentage of inaccuracy is also displayed.

4.1 Bracket plate (model 1)

The first model for the two-dimensional plane stress problem is illustrated in Figure 4(a). In this case, a bracket plate section is constrained in both x and y directions at the left vertical edge, and a uniform tensile stress of 1000 psi is applied perpendicular to the bottom one-fourth portion of the plate at the right vertical edge. In this model, the useful values are:

Uniform stress at the edge	σ = 1000 psi
Thickness of the plates	t = 0.05 inch
Modulus of Elasticity	$E = 10 \times 10^6$ psi
Poisson's ratio	$\upsilon = 0.3$
Diameter of the hole	d = 1.5 inch
Bracket radius	r = 1.0 inch

Figure 4(b) depicts the boundary conditions and loadings that are being applied. In this illustration, the left vertical edge of the bracket section is limited in both x and y directions, i.e., $Ux = Uy = 0$, with a uniform tensile stress of 1000 psi acting perpendicular to the bottom one-fourth part of the plate at the right vertical edge. There are 284 nodes and 239 quadrilateral elements in the model. Figure 4(c) shows the generated quadrilateral mesh for the bracket plate section.

Figure 5(a) shows the FEM analysis results of model 1 in terms of σ_{mises} (von Mises stress). As shown in Figure 5(b), the von Mises stress is maximum around the location of element no. 6, notably around the nodes 14 and 15. The output file for model 1 in terms of stresses at the four integration points is obtained using a developed program for plane stress analysis. It is clear from Figure 5(b) that the von Mises stress is maximum for element no. 6 (most vulnerable region), which includes nodes 14, 15, 103, and 273. Table 1 through Table 4 show the comparison of σ_{mises}, σ_x, σ_y, and τ_{xy} for element no. 6 at the four integration points derived from the developed program and the finite element analysis software.

While comparing σ_{mises} (von Mises stresses), it is obvious from Table 1 that the maximum tensile stress is found at the integration point 4 (node no. 273) for element no. 6 which has a value of 26176.5 psi obtained from the developed

program and 26176.6 psi derived from the analysis. These two values are quite identical, having an error of 0.001%. All the stresses are tensile. By comparing all these values in Table 1, the results of σ_{mises} are very close showing relatively small percentage of error in the range of 0.001-0.005%. Similar results of σ_{mises} were observed in these studies (Hoque, 2016; Hoque and Islam, 2023).

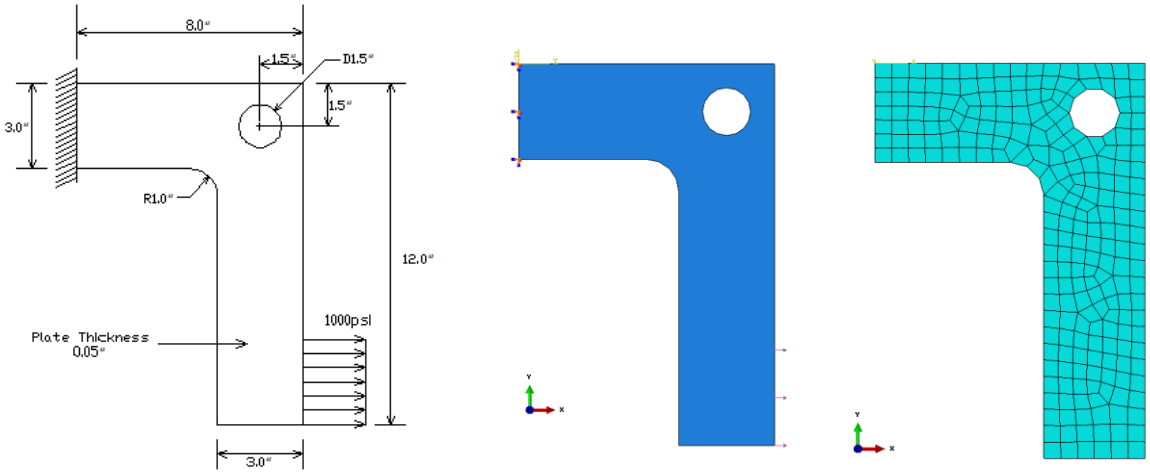

(a) (b) (c)

Figure 4: a) Bracket plate (model 1); b) Application of boundary conditions and loadings (model 1); c) Quadrilateral mesh (model 1)

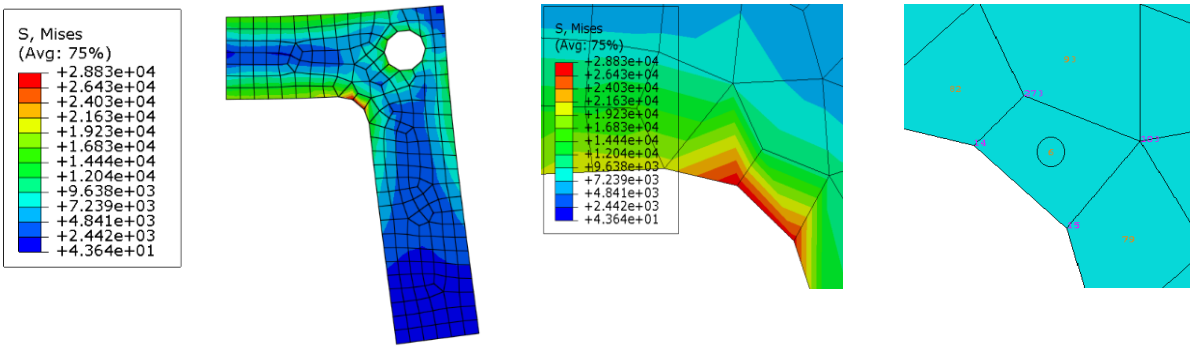

(a) (b)

Figure 5: a) FEM analysis of model 1 in terms of σ_{mises}; b) Location of most vulnerable region of model 1 in terms of σ_{mises} (element no. 6)

Table 1: Comparison of σ_{mises} for model 1

Element No.	Integration point (Node No.)	σ_{mises} from developed program (psi)	σ_{mises} from analysis (psi)	% of error
6	1(14)	18050.8	18050.4	0.002
	2(15)	14934.5	14933.7	0.005
	3(103)	25936.1	25936.3	0.001
	4(273)	26176.5	26176.6	0.001

Table 2: Comparison of σ_x for model 1

Element No.	Integration point (Node No.)	σ_x from developed program (psi)	σ_x from analysis (psi)	% of error
6	1(14)	7925.1	7924.5	0.007
	2(15)	10670.1	10669.8	0.003
	3(103)	19691.7	19692.2	0.003
	4(273)	14852.3	14852.2	0.001

Table 3: Comparison of σ_y for model 1

Element No.	Integration point (Node No.)	σ_y from developed program (psi)	σ_y from analysis (psi)	% of error
6	1(14)	11500.6	11500.5	0.001
	2(15)	4448.4	4447.8	0.013
	3(103)	12137.9	12138.0	0.001
	4(273)	17109.0	17109.3	0.002

Table 4: Comparison of τ_{xy} for model 1

Element No.	Integration point (Node No.)	τ_{xy} from developed program (psi)	τ_{xy} from analysis (psi)	% of error
6	1(14)	-8600.5	-8600.3	0.002
	2(15)	-6754.3	-6753.9	0.006
	3(103)	-11204.2	-11204.2	0
	4(273)	-11916.5	-11916.5	0

* (+) stress value indicates tensile stress, whereas (-) stress value represents compressive stress.

From the values of σ_x (normal stresses along x-direction), it is seen from Table 2 that the maximum tensile stress is found at the integration point 3 (node no. 103) for element no. 6 which has a value of 19691.7 psi generated from the developed program and 19692.2 psi derived from the analysis. These two values are quite closer having an error of 0.003%. It is observed that all the stresses are tensile. When compared to the other stress values in Table 2, the findings of σ_x are practically equal, indicating a minimal percentage of error ranged between 0.001-0.007%.

Table 3 represents σ_y (normal stresses along y-direction) in which the maximum tensile stress is determined at the integration point 4 (node no. 273) for element no. 6 with a value of 17109.0 psi generated from the developed program and 17109.3 psi derived from the analysis. These two quantities are nearly identical, with a 0.002% of error. All the stresses are found to be tensile in nature. When all these values in Table 3 are compared, σ_y 's results are quite consistent, with a little percentage of error in the range of 0.001-0.002%.

In case of τ_{xy} (shear stresses), Table 4 shows that the compressive stress for element no. 6 is maximum at the integration point 4 (node no. 273), with a value of 11916.5 psi procured from the developed program and 11916.5 psi derived from the analysis. These two values are identical, which is remarkable. The remaining stress values are all

compressive. When compared to the other stress values in Table 4, it is evident that the τ_{xy} (shear stress) findings are almost similar, with a little percentage of error ranging from 0.002-0.006%.

The von Mies stress is maximum around the region of element no. 6, particularly near the nodes 14 and 15, as shown in Figure 5(b). With the aid of a developed program for plane stress analysis, the output file for model 1 in terms of stresses at the four integration points is obtained. The von Mises stress is maximum for element no. 6 (most vulnerable region), which includes nodes 14, 15, 103, and 273, as shown in Figure 5(b). The comparison of σ_{mises}, σ_x, σ_y, and τ_{xy} for element no. 6 at the four integration points obtained from the developed program and the finite element analysis software are shown in Tables 1 through Table 4. For instance, if node no. 273 of element no. 6 is considered, the von Mises stress is found to be 26176.5 psi from the developed program (theoretical). This von Mises stress value is a geometrical combination of all stresses acting at a certain location i.e., normal stress in two-directions and shear stress. For node no. 273 of element no. 6, the normal stresses along x & y direction and shear stress are found to be 14852.3 psi, 17109.0 psi, and -11916.5 psi respectively. Using these values of normal stress and shear stress and by applying Equation (7), the von Mises stress of 26176.5 psi is obtained from theoretical formulation. The von Mises stress of 26176.6 psi is obtained from the analysis as well. These two von Mises stress values are almost identical, showing only 0.001% of error. While the von Mises stress values for other nodes (node no. 14, 15, 103) of element no. 6 obtained from the developed program are compared with the analysis results, it is observed that the results depict very small percentage of error ranging from 0.001-0.005%. Therefore, it can be said that the results of the developed program agree quite well with the analysis results. The material used for model 1 is aluminum, whose yield strength is 40000 psi. According to the criterion of von Mises stress, it should not exceed the yield strength of the material, otherwise the material yields and ruptures at that place. The von Mises stress values obtained from the developed program and from the analysis for the four nodes (node no. 14, 15, 103, and 273) of element no. 6 are within the range of yield strength (i.e., less than the yield strength) of that material. Therefore, it can be said that the bracket plate (model 1) won't yield and sustain under the application of a uniform tensile stress at the edge.

4.2 L-shaped plate (model 2)

The second model represents a two-dimensional plane strain problem as illustrated in Figure 6(a). In this model, an L-shaped plate section is constrained at the left vertical edge in both x and y direction and a uniform compressive stress of 1000 psi is applied in a perpendicular direction to the horizontal edge as shown in Figure 6(a). In this case, the useful quantities are:

Uniform stress at the edge	$\sigma = 1000$ psi
Length of the plate	$L = 20$ in.
Modulus of Elasticity	$E = 30 \times 10^6$ psi
Poisson's ratio	$\upsilon = 0.25$

In Figure 6(b), the boundary conditions and loadings are imposed. Figure 6(b) shows that the L-shaped plate section's left vertical edge is constrained in both x and y directions, i.e., $U_x = U_y = 0$, and that a uniform compressive stress acting perpendicular to the top half part at the right horizontal edge of the plate is 1000 psi.

For fine mesh, the model has 2239 nodes and 2148 quadrilateral elements. The model is modified in terms of aspect ratios to develop coarse mesh. As a result, the model has 175 nodes and 150 quadrilateral elements for the coarse mesh. The generated quadrilateral mesh (both fine mesh and coarse mesh) for the above model is illustrated in Figure 7(a) and Figure 7(b) respectively.

Figure 8(a) shows the FEM analysis results of model 2 (fine mesh) in terms of σ_{mises} (von Mises stress). As shown in Figure 8(b), the von Mises stress is maximum around the region of element no. 439, notably around the nodes 99 and 100. The output file for model 2 in terms of stresses at the four integration points is obtained using a developed program for plane strain analysis. It is clear from Figure 8(b) that the von Mises stress is maximum for element no. 439 (most vulnerable region), which includes nodes 99, 100, 480, and 483.

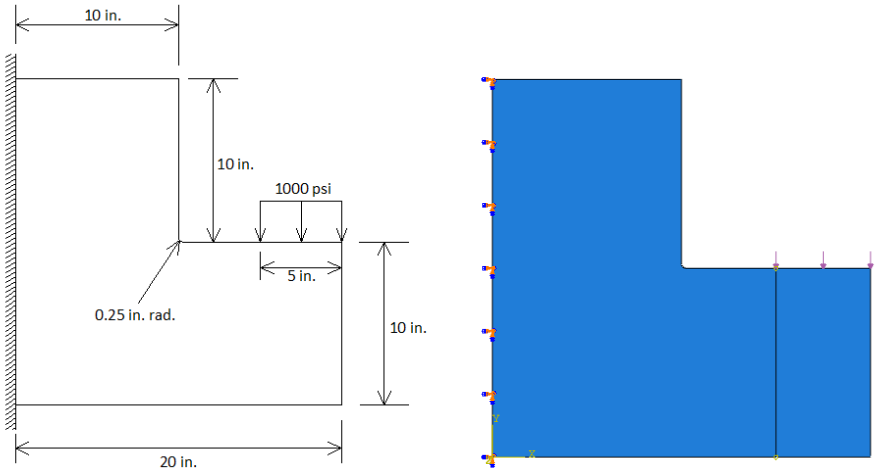

(a) (b)

Figure 6: a) L-shaped plate (model 2); b) Application of boundary conditions and loadings (model 2)

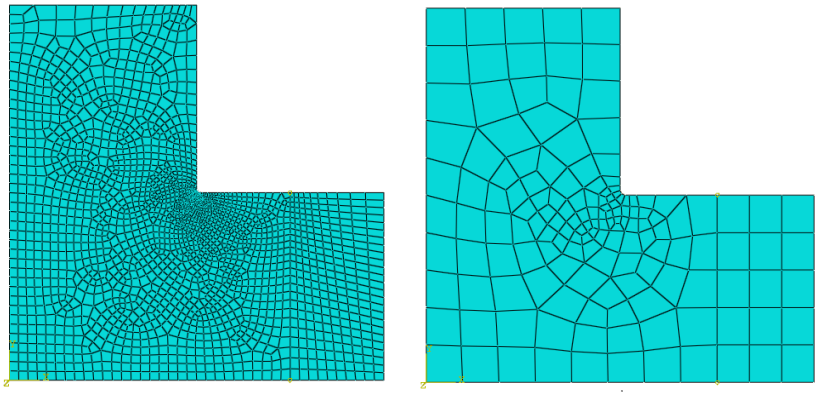

(a) (b)

Figure 7: a) Quadrilateral mesh for model 2 (fine mesh); b) Quadrilateral mesh for model 2 (coarse mesh)

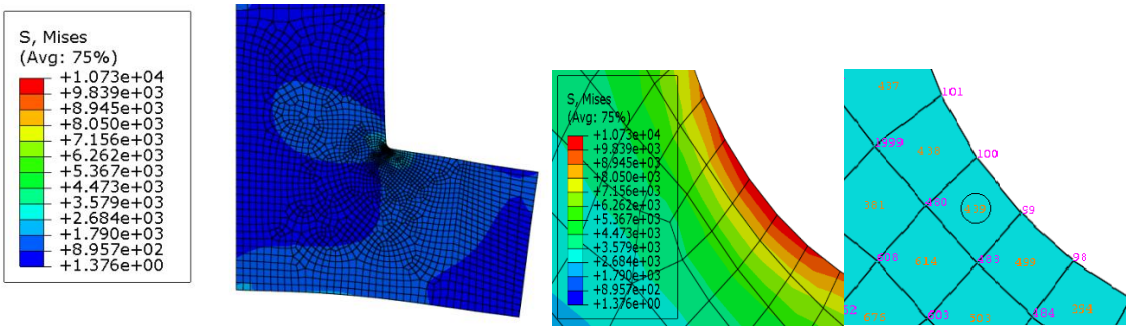

(a) (b)

Figure 8: a) FEM analysis of model 2 (fine mesh) in terms of σ_{mises}; b) Location of most vulnerable region of model 2 (fine mesh) in terms of σ_{mises} (element no. 439)

Model 2 (coarse mesh) FEM analysis findings in terms of σ_{mises} (von Mises stress) are shown in Figure 9(a). The von Mises stresses are maximum near the region of element no. 44 which consists of nodes 6, 26, 61, 67 and element no. 27 which comprises node no 5, 26, 66, 67, as seen in Figure 9(b). A developed program for plane strain analysis is used to generate the output file for model 2 in terms of stresses at the four integration points.

As von Mises stress is a combination of normal and shear stresses in all directions, so for the analysis purpose, the results of von Mises stress of model 2 (fine mesh as well as coarse mesh) are compared at the most vulnerable region. Table 5 through Table 6 show the comparison of σ_{mises} for element no. 439 (fine mesh) and element no. 27 & 44 (coarse mesh) at the four integration points derived from the developed program and the finite element analysis software. The most vulnerable region for fine mesh is element no. 439, while the most vulnerable location for coarse mesh is element no. 27 and 44.

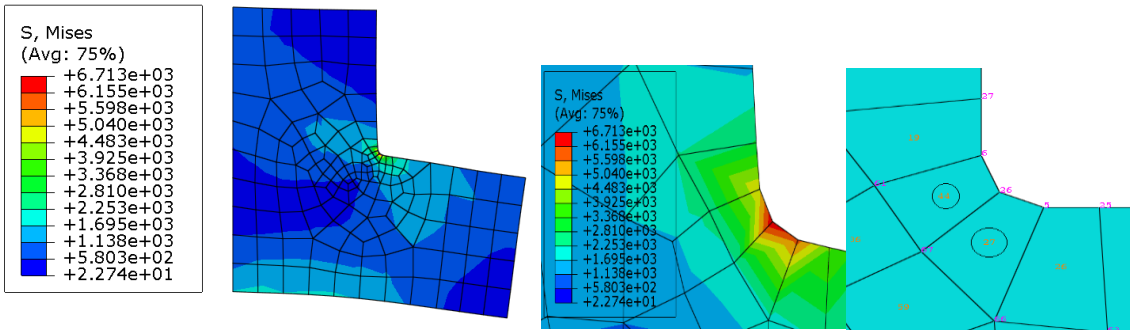

(a) (b)

Figure 9: a) FEM analysis of model 2 (coarse mesh) in terms of σ_{mises}; b) Location of most vulnerable region of model 2 (coarse mesh) in terms of σ_{mises} (element no. 27 & 44)

While comparing σ_{mises} (von Mises stresses) for model 2 (fine mesh), it is obvious from Table 5 that the maximum tensile stress for element no. 439 is found at the integration point 2 (node no. 99), that has a value of 11672.6 psi computed from the developed program and 10110.5 psi derived from the analysis. These two numbers represent a 13.383% of error. The minimum tensile stress for element no. 439 is determined at the integration point 1 (node no. 483), with a value of 9759.9 psi computed from the developed program and 8896.2 psi obtained from the analysis. There is an inaccuracy of 8.850% between these two values. While looking at the other stress values in Table 5, it is evident that the results of σ_{mises} are comparable, with an error of roughly 8.850-13.717%. This is quite significant. σ_{mises}' findings were remarkably comparable to those studies (Hoque, 2016; Hoque and Islam, 2023).

Table 5: Comparison of σ_{mises} for model 2 (fine mesh)

Element No.	**Integration point (Node No.)**	**σ_{mises} from developed program (psi)**	**σ_{mises} from analysis (psi)**	**% of error**
439	1(483)	9759.9	8896.2	8.850
	2(99)	11672.6	10110.5	13.383
	3(100)	11647.7	10050.0	13.717
	4(480)	9798.5	8881.2	9.362

Table 6 represents comparison of σ_{mises} (von Mises stresses) for model 2 (coarse mesh). From Table 6, it is noted that the maximum tensile stress is found at the integration point 1 (node no. 26) for element no. 44, with a value of 7097.1 psi computed from the generated program and 5535.8 psi derived from the analysis. These two numbers illustrate a 21.999% inaccuracy. The minimum tensile stress, on the other hand, is determined at the integration point 4 (node no. 67) for element no. 27, with a value of 3053.7 psi obtained from the developed program and 2831.4 psi derived from the analysis. The difference between these two values is 7.281%. When all other stress values in Table 6 are compared,

it is observed that the results of σ_{mises} obtained from the developed program and the analysis range from 4.377-21.999%, which is quite significant.

Table 6: Comparison of σ_{mises} for model 2 (coarse mesh)

Element No.	Integration point (Node No.)	σ_{mises} from developed program (psi)	σ_{mises} from analysis (psi)	% of error
27	1(66)	3360.0	3025.1	9.968
	2(5)	6594.8	5340.9	19.014
	3(26)	6784.3	5340.9	21.276
	4(67)	3053.7	2831.4	7.281
44	1(26)	7097.1	5535.8	21.999
	2(6)	6311.5	5168.2	18.115
	3(61)	3103.1	2967.2	4.377
	4(67)	3589.0	3224.5	10.158

It should be mentioned that the findings from the developed program and the analysis ranged from roughly 8.850–13.717% when comparing σ_{mises} for model 2 with fine mesh. Contrarily, the results for model 2 with coarse mesh ranged from 4.377 to 21.999%. In other words, fine mesh generates more accurate findings than those of coarse mesh. The computational results of fine mesh are significantly more reliable than those of coarse mesh. As a result, it is obvious that as the mesh gets finer, the proportion of inaccuracy in the theoretical and computational solutions should go smaller. A convergence test is not necessary when analyzing the stresses for different models of plane stress and plane strain problems because the main objective of this study is to compare the findings gained from the developed program to the results obtained from the analysis.

The von Mises stress, which consists of normal stress occurring in two directions and shear stress, is a geometric combination of all stresses acting at a particular location. von Mises stress values obtained from the developed program and analysis for both fine mesh (element no. 439) and coarse mesh (element no. 27 and 44) indicate an error of 8.850-13.717% for fine mesh and 4.377-21.999% for coarse mesh, which is quite comparable. Therefore, it can be said that the results of the developed program (theoretical) agree quite well with the findings obtained from the analysis. A mild steel with a yield strength of 48000 psi was used to manufacture model 2. The material must not be subjected to a stress greater than its yield strength to avoid the material yielding and breaking at that location, which is a requirement of the von Mises stress criterion. The von Mises stress values found by the developed program and by analysis for the most vulnerable spot of both fine mesh and coarse mesh are within the limit of yield strength (i.e., less than the yield strength) of that material. It follows that the L-shaped plate (model 2) didn't yield and withstand under the application of a uniform tensile stress at the edge.

A research work was conducted on the model experiment of large superstructures' influence on hull girder ultimate strength for cruise ships by Shi and Gao (Shi and Gao, 2021). In this work of Shi and Gao, non-linear finite element analysis was performed on cruise ship models with superstructures. The analysis was conducted on three-dimensional models. Shell element (six nodes) was used for analysis purposes. The stress values obtained from the analysis were compared with the experimental results. However, in this study, two-dimensional plate sections with structural discontinuities such as a plate with holes, plate with bracket and holes, and plate with fillets were developed for analysis purpose. The problems are associated with two-dimensional plan stress and plane strain issues, in which quadrilateral elements (four nodes) are used for analysis purpose. The values of stress obtained from the analysis are compared with the findings derived from the developed program. Though the program is developed for two-dimensional plane stress and plane strain problems, a three-dimensional program is still in progress which can be

applicable to any three-dimensional models to generate nodal displacement and nodal stress values, and those results can be compared with the analysis findings as well as the experimental results.

5. Conclusions

The following are the findings that can be drawn from this research:

- For two-dimensional four node quadrilateral elements, a reliable object-oriented program is developed that can effectively provide the value of normal stress, shear stress, and von Mises stress at the four integration points for various ship structures with structural discontinuity, such as plate with holes, plate with bracket and holes etc. This application may be used to solve a variety of two-dimensional plane stress and plane strain problems.
- The finding of this research validates the gauss point stresses produced from the developed program at the most vulnerable region of various ship structures. When all these gauss point stress values are compared, it is evident that the findings obtained from the developed program and the analysis are almost similar, with a minimal percentage of error.
- When comparing von Mises stresses for fine mesh, the findings produced from the developed program and the analysis differ by roughly 8-13%. von Mises stresses, on the other hand, vary between 4-21% for coarse mesh. This means that fine mesh produces more accurate findings than coarse mesh. The proportion of inaccuracy produced from theoretical and computational findings should be less as the mesh grows finer. Because the aim of the work is to compute the results of the developed program and compare them to the findings of the analysis, convergence testing is not required when assessing stresses and displacements for various plane stress and plane strain problems.
- The findings of structural discontinuities associated with ship structures for two-dimensional plane stress problems utilizing finite element analysis software are better understood in this work.

Acknowledgements

I would like to appreciate everyone who have assisted me directly or indirectly during several stages of the work. In addition, regarding the simulation lab facilities, I would like to draw attention to the UGC HEQEP Sub Project "Strengthening the Research Capabilities and Experimental Facilities in the Field of Marine Structure" (CP#3131).

References

Baumann, G.W. (1997): Linear structural stress analysis of a hull girder penetration and a short longitudinal bulkhead using finite element modeling. M.Sc. Thesis, Naval Postgraduate School, Monterey, California, USA.

Bea, R.G., Cramer, E., Schulte-Strauthaus, R., Mayoss, R., Gallion, K., Ma, K., Holzman, R., and Demsetz, L. (1995): Ship's Maintenance Project. Conducted at University of California, Berkeley for US Coast Guard, Ship Structure Committee (SSC), SSC-386.

Desjardins, R., and Fafard, M. (1992): Developpement d'un logiciel pour I'analyse des structures par elements finis utilisant l'approche de la programmation orientee objets. Rapport GCT-92-05, Universite Laval, Sainte-Foy, Canada.

Dubois-Pelerin, Y., Zimmermann, T., and Bomme, P. (1992): Object-oriented finite element programming, A prototype program in Smalltalk. Comput. Methods Appl. Mech. Engrg. 98, pp. 361-397.

Edholm, A. (2013): Meshing and visualization routines in the python version of CALFEM. Master's Dissertation, Lund University, Sweden.

Fenves, G.L. (1990): Object-oriented programming for engineering software development. Engrg. with Comput. 6, pp. 1-15.

Forde, B.W.R., Foschi, R.O., and Stiemer, S.F. (1990): Object-oriented finite element analysis. Comput. & Structures 34, pp. 355-374.

Hoque, K. N., and Presuel-Moreno, F. (2023): Accelerated Corrosion of Steel Rebar in Concrete by Electromigration: Effect of Reservoir Length and Concrete Mixes. Proceedings of the 13th International Conference on Marine Technology (MARTEC 2022). https://doi.org/10.2139/ssrn.4446360

Hoque, K. N., and Presuel-Moreno, F. (2023): Corrosion Propagation of Steel Rebar Embedded in Marine Structures Prepared with Binary Blended Concrete Containing Slag. Proceedings of the 13th International Conference on Marine Technology (MARTEC 2022). https://doi.org/10.2139/ssrn.4447455
Hoque, K. N., and Presuel-Moreno, F. (2023): Corrosion Behavior of Reinforcing Steel Embedded in Fly Ash Concrete. Proceedings of the 13th International Conference on Marine Technology (MARTEC 2022). https://doi.org/10.2139/ssrn.4447479
Hoque, K. N., and Presuel-Moreno, F. (2023): Corrosion of Steel Rebar Embedded in Ternary Blended Concrete Exposed to High Humidity Environment. Proceedings of the 13th International Conference on Marine Technology (MARTEC 2022). https://doi.org/10.2139/ssrn.4447482.
Hoque, K. N., and Islam, M. S. (2023): Finite Element Approach to Analyze Structural Discontinuities Associated with Ship Hull. Proceedings of the 13th International Conference on Marine Technology (MARTEC 2022). https://doi.org/10.2139/ssrn.4447483
Hoque, K. (2020): Corrosion propagation of reinforcing steel embedded in binary and ternary concrete. Ph.D. Dissertation, Department of Ocean and Mechanical Engineering, Florida Atlantic University (FAU), Boca Raton, Florida, USA.
Hoque, K. (2016): Analysis of structural discontinuities in ship hull using finite element method. M.Sc. Thesis, Department of Naval Architecture and Marine Engineering, Bangladesh University of Engineering and Technology (BUET), Dhaka, Bangladesh.
Islam, M. S., and Paul, S. C. (2021): Topology optimization of an oil tanker bulkhead subjected to hydrostatic loads. Journal of Naval Architecture and Marine Engineering (JNAME), Vol. 18, pp. 207-215.
Islam, M.S., Kabir, M.H., and Paul, S.C. (2017): Simulation-based structural analysis of an oil tanker bulkhead. Procedia Engineering, 194:517–521.
Kar, S., Sarangdhar, D.G., and Chopra, G.S. (2008): Analysis of ship structures using ANSYS, ANSYS Conference.
Mackerle, J. (2000): Object-oriented techniques in FEM and BEM. a bibliography (1996-1999), Finite Elements in Analysis and Design, Vol. 36, pp. 189-196.
Martha, L.F. (2002): An object-oriented framework for finite element programming. in Fifth World Congress on Computational Mechanics, Austria.
Miller, G.R. (1991): An object-oriented approach to structural analysis and design. Comput. & Structures 40, pp. 75-82.
Niu, M.C. (1998): Airframe Structural Design. Conmilit Press Ltd., Hong Kong.
Parunov, J., Uroda, T., and Senjanovic, I. (2010): Structural analysis of a general cargo ship, Brodogradnja, 61-1, 28-33.
Presuel-Moreno, F., Hoque, K., and Rosa-Pagan, A. (2022): Corrosion propagation monitoring using galvanostatic pulse on reinforced concrete legacy samples. 2020-FAU-02 Final Report for National University Transportation Center TriDurLE.
Presuel-Moreno, F., and Hoque, K. (2019): Corrosion propagation of carbon steel rebar embedded in concrete. NACE Corrosion 2019 Conference & Expo, Nashville, Tennessee, USA.
Presuel-Moreno, F., Nazim, M., Tang, F., Hoque, K., and Bencosme, R. (2018): Corrosion propagation of carbon steel rebars in high performance concrete. BDV27-977-08 Final Report for Florida Department of Transportation (FDOT) Research Center.
Shi, G.J., and Gao, D.-W. (2021): Model experiment of large superstructures' influence on hull girder ultimate strength for cruise ships. Ocean Engineering, Vol. 222, pp. 1-10.
Soares, C.G., and Garbatov, Y. (1998): Reliability of maintained ship hull girders subjected to corrosion and fatigue. Struct. Saf. 20, pp. 119-201.
Strebel, J.J., and Moet, A. (1993): Plane strain and plane stress analysis of fatigue crack propagation in medium density polythylene pipe materials. Polymer Engineering and Science, Vol. 33, Issue 4, pp. 217-226.
Zimmermann, T., Dubois-Pelerin, Y., and Bomme, P. (1992): Object-oriented finite element programming, Governing principles. Comput. Methods Appl. Mech.